

Potential of Time Correlation to Improve Limits of Detection in Inductively Coupled Plasma-Atomic Emission Spectrometry

J.M. Mermet

Contribution from: Laboratoire des Sciences Analytiques, Bat-CPE, Université Claude Bernard-Lyon 1, 69622 Villeurbanne Cedex, France

Received: September 10, 2004

Accepted (in revised form): November 19, 2004

Résumé

La définition de la limite de détection selon l'IUPAC a été adaptée à la possibilité d'obtenir une corrélation temporelle entre des signaux, en utilisant une détection multicanal en spectrométrie d'émission atomique avec un plasma à couplage inductif. Les fluctuations du fond peuvent être minimisées en soustrayant deux signaux du fond corrélés temporellement, si le système est limité par le bruit de scintillation, c'est à dire que les bruits dus aux photons, bruit de grenaille et bruits du détecteur, sont négligeables par rapport au bruit de scintillation. Ce peut être obtenu en sélectionnant des longs temps d'intégration (> 10 s), et en utilisant des conditions opératoires et instrumentales fournissant une intensité élevée du fond. Des travaux préliminaires ont conduit à obtenir des améliorations de la limite de détection jusqu'à 5, en utilisant les meilleures conditions.

Abstract

The IUPAC definition of the limit of detection has been adapted to the possibility of having time correlation between signals when using multichannel detection in inductively coupled plasma-atomic emission spectrometry. Minimization of the background fluctuations can be obtained by subtracting two time-correlated background signals, provided that the system is flicker-noise limited, i.e. the photon-related noises such as shot noise and detector noises are negligible in comparison to flicker

noise. This can be obtained by using long integration times (> 10 s) and by using operating and instrument conditions that provide a high background intensity. Preliminary investigations led to a LOD improvement of up to 5 under the most favourable conditions.

Keywords: Inductively coupled plasma, atomic emission spectrometry, IUPAC limit of detection, time correlation.

Introduction

When dealing with the estimation of limit of detection (LOD), most publications in the field of atomic spectrometry refer to the IUPAC approach, *i.e.* based on the signal-to-noise ratio (SNR) (1). The LOD, c_L , is given by:

$$c_L = \frac{k \cdot s_B \cdot c}{S} \quad (1)$$

where k is a statistical coefficient, usually equal to 3, s_B is the estimation of the standard deviation of the background fluctuations, and S is the net signal obtained for a given concentration, c . The net line intensity S is obtained by subtracting the background intensity B from the gross line intensity, X , *i.e.* $S = X - B$. Actually, though first described for atomic spectroscopy, this LOD definition is widely used, regardless of the analytical method.

Improving LODs has always been a challenge in analytical chemistry, and it is generally done by either increasing the signal for a given concentration or by decreasing the background noise. In ICP-AES, an increased signal (or signal-to-background ratio) may be obtained by using, for instance, axial viewing, ultrasonic

* Author to whom correspondence should be addressed: mermet@cpe.fr

nebulization, high resolution (2) or signal addition. Signal addition is facilitated by the use of multichannel detection, which is currently based on charge transfer device (CTD) detectors, either of the charge-coupled device (CCD) or charge-injected device (CID) type (3-7). The concept is to replace the net signal intensity, S , in equation (1) by the addition of two lines, S_1 and S_2 , and of two backgrounds, B_1 and B_2 . S and s_B are replaced by S_{res} and $s_{B,res}$, respectively. Equation (1) becomes

$$c_L = \frac{k \cdot s_{B,res} \cdot c}{S_{res}} \quad (2)$$

The ideal case is when $S_1 = S_2$ and $s_{B,1} = s_{B,2}$. We have then:

$$s_{B,res} = \sqrt{2} s_{B,1} \quad (3)$$

and

$$c_L = \frac{k \cdot c \cdot s_{B,1}}{\sqrt{2} S_1} \quad (4)$$

The best improvement is, therefore, only 1.4. Obviously, if $S_2 < S_1$, the improvement would be less; in other words, it would not be worthwhile to use this procedure. It could be thought that the addition of a larger number of lines would provide a better improvement in the LOD. For instance, Cr exhibits a large number of sensitive ionic lines (table 1). If the first 10 sensitive lines are taken into account, and the most sensitive line intensity (Cr II 283.564) is S_1 , then $S_{res} = 5.15 S_1$, and the LOD is only improved by $5.15/\sqrt{10}$, *i.e.* 1.6. Clearly, line addition does not lead to a significant improvement in the LOD.

An alternative is the reduction of the standard deviation of the background fluctuations, which is possible by increasing the photon acquisition time, so that the standard deviation due to the shot noise is minimized. Another possibility would be the use of time correlation between background intensities to reduce background fluctuations.

Most analysts will use the IUPAC LOD definition by determining the signal S corresponding to the concentration c with a limited number of replicates. In contrast, at least 10 replicates are used to determine the standard deviation of the background. This implies that the signal and the background are measured in a sequential way. Although not excluded, nothing was mentioned in

Table 1. List of the ten most sensitive Cr II lines, with the net intensity, S , normalized to the most intense line (Cr II 283.564 nm). The intensity sum is equal to 5.15. The experiment was performed on a Varian Pro ICP-AES system (1500 W, with a carrier gas flow rate of 0.8 L min⁻¹).

nm	S
283.564	1.00
267.719	0.82
284.324	0.73
267.713	0.61
276.655	0.47
284.983	0.36
313.205	0.35
205.560	0.33
312.495	0.25
276.258	0.24

the IUPAC procedure concerning the possibility of reducing background noise by using time correlation between noise signals. This was probably justified at the time of the publication, when background was never truly measured simultaneously with either the analyte line or with another background. In ICP-AES, so-called simultaneous systems, *i.e.* polychromators equipped with photomultiplier tubes, have been made commercially available since the very beginning of the technique. However, simultaneous measurements were mostly used for analyte signal intensities, in order to increase the speed of analysis. Background measurements were usually performed by either moving the entrance slit, or by rotating a refractory plate, both devices being used to scan the line profile and its vicinity. Consequently, background measurements were conducted at a time different from that of the line intensity measurements.

However, simultaneous measurements between lines were not only used to increase sample throughput, but also to improve repeatability. This possibility is one of the major features of CTD-based simultaneous measurements that led to a significant improvement in repeatability, provided that the measurement was flicker noise limited (8,9).

It should be noted that, in one of the early works on PMT-based simultaneous measurements, signal correlation between different background intensities had been obtained under specific operating conditions, *i.e.*,

long integration times and large spectral windows (10). However, the dispersive system was a monochromator, and it was necessary to add a second dispersive system to obtain the possibility of simultaneous measurements.

Time correlation has already been used to improve LODs; however, this was done by following a different approach, namely by using the relative standard deviation (RSD) of the net signal, RSD_{net} , *i.e.* the signal after background subtraction (11-17). In this case, time correlation between the analyte line intensity and the adjacent background intensity is used. It was shown that an improvement up to a factor of 10 could be obtained. Although the RSD_{net} approach is used, for instance, in separation methods (18), the vast majority of ICP-AES users still uses the IUPAC approach. The aim of this work is, therefore, to describe the benefits of time correlation in noise reduction, to adapt time correlation to the IUPAC LOD approach, to optimize the operating conditions, and to raise the current limitations.

Evaluation of the correlation factor

When two distributions of the n variables a and b exhibit standard deviations, σ_a and σ_b , and means \bar{a} and \bar{b} , respectively, the resultant standard deviation σ_{res} of the two combined distributions is given by:

$$\sigma_{res}^2 = \sigma_a^2 + \sigma_b^2 - 2\text{cov}(a,b) \quad (5)$$

with:

$$\text{cov}(a,b) = \frac{1}{n-1} \sum_{i=1}^n (a_i - \bar{a})(b_i - \bar{b}) \quad (6)$$

The correlation factor, θ , is given by:

$$\theta = \frac{\text{cov}(a,b)}{\sigma_a \sigma_b} \quad (7)$$

Eqn. (5) becomes:

$$\sigma_{res}^2 = \sigma_a^2 + \sigma_b^2 - 2 \times \theta \times \sigma_a \times \sigma_b \quad (8)$$

From the experimental values of σ_{res} , σ_a and σ_b , it is then possible to deduce the value of θ . Note that a spreadsheet software like Excel provides the value of θ for two series of data. For signals with different intensities, the values of σ_a and σ_b will have different magnitude.

If $\sigma_a \neq \sigma_b$, *i.e.* $\sigma_b = \sigma_a + d$, equation (8) can be written:

$$\sigma_{res}^2 = 2 \times \sigma_a (\sigma_a + d) (1 - \theta) + d^2 \quad (9)$$

This means that, even if $\theta = 1$, σ_{res} is not equal to 0, but to d .

A better case is obtained when $\sigma_a = \sigma_b = \sigma_{exp}$. Equation (8) can be then written:

$$\sigma_{res}^2 = 2 \times \sigma_{exp}^2 - 2 \times \theta \times \sigma_{exp}^2 \quad (10)$$

or

$$\sigma_{res}^2 = 2(1 - \theta) \sigma_{exp}^2 \quad (11)$$

When $\theta = 0$, no correlation is observed, and the two fluctuations are independent. Correlation and negative correlations are observed for $\theta = 1$ and $\theta = -1$, respectively. A (positive) correlation is observed when the two simultaneous signals exhibit the same shape, while a negative correlation is observed when the two signals exhibit an opposite shape. The resulting σ_{res} will depend on i) the type of correlation, *i.e.* positive or negative; and ii) the way the two signals are combined. Equation (11) may be written:

$$\sigma_{res}^2 = 2(1 - g \times \theta) \sigma_{exp}^2 \quad (12)$$

where $g = 1$ for subtraction and division, and $g = -1$ for addition or multiplication.

Therefore, in the case of the subtraction of the two signals (or division), we have the following possibilities :

- negative correlation : $g\theta \rightarrow -1$, and $\sigma_{res} \rightarrow 2\sigma_{exp}$
- no correlation : $g\theta = 0$, and $\sigma_{res} = \sqrt{2}\sigma_{exp}$
- correlation : $g\theta \rightarrow 1$, and $\sigma_{res} \rightarrow 0$

In the case of the addition of the two signals (or multiplication), we have the following possibilities :

- correlation : $g\theta \rightarrow -1$, and $\sigma_{res} \rightarrow 2\sigma_{exp}$
- no correlation : $g\theta = 0$, and $\sigma_{res} = \sqrt{2}\sigma_{exp}$
- negative correlation : $g\theta \rightarrow 1$, and $\sigma_{res} \rightarrow 0$

Time-correlated combination of lines and backgrounds

The concept is to replace the intensity and the standard deviation of a single line by the addition or subtraction of i) two lines S_a and S_b , and ii) the estimations of the two standard deviations, s_a and s_b .

Addition of two time-correlated lines and backgrounds

In this case, and assuming $S_b = S_a$, s_{res} is equal to :

$$s_{res} = \sqrt{2(1 - g \times \theta)} s_a \quad (13)$$

where θ is the correlation factor.

$$c_L = \frac{3 \cdot c \cdot \sqrt{2(1 - g \times \theta)} \cdot s_a}{2 \cdot S_a} \quad (14)$$

Because the two signals are correlated, θ tends to 0 and, due to the signal addition, $g = -1$. For $\theta = 0.8$, $g\theta = -0.8$, and the improvement factor is 1.05, and when $g\theta = -0.99$, the factor is 1. There is, therefore, no improvement by adding lines with time correlation.

Subtraction of two time-correlated lines and backgrounds

If we subtract two lines, we have :

$$S_{res} = (X_a - B_a) - (X_b - B_b) \quad (15)$$

Obviously, if $X_a = X_b$, there is no benefit, as the resulting signal, S_{res} is equal to 0. The key point to adapt time correlation to the IUPAC definition is to select a line S_b so weak that the net line intensity, X_b , may be assimilated to the background B_b (figure 1). In this case, we can write that $X_b = B_b$, and then $S_{res} = X_a - B_a = S_a$.

The LOD becomes

$$c_L = \frac{3 \cdot c \cdot \sqrt{2(1 - \theta)} \cdot s_a}{S_a} \quad (16)$$

The LOD improvement factor is, therefore :

$$\frac{1}{\sqrt{2(1 - \theta)}} \quad (17)$$

When $\theta = 0.80, 0.90, 0.95, 0.99$ and 0.995 , the improvement factor is 1.6, 2.2, 3.2, 7.1 and 10.0, respectively.

Operating conditions to obtain time correlation

In order to obtain a high correlation factor, the noises of the two background intensities should be highly correlated. This correlation will depend on the predominant noise. It is convenient to express the noise of the background as a relative standard deviation, RSD_B . In the case of CTD detectors, we have (7):

$$RSD_B = \left[\alpha_B^2 + \frac{1}{z_B \cdot \tau_i} + \frac{z_{dark}^2}{z_B^2 \cdot \tau_i} + \frac{\sigma_{ro}^2}{z_B^2 \cdot \tau_i^2} \right]^{1/2} \quad (18)$$

where α_B is the flicker noise coefficient, z_B is the background intensity expressed in $e \text{ pixel}^{-1} \text{ s}^{-1}$, τ_i is the

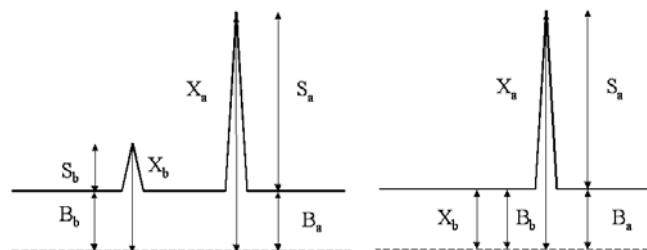


Figure 1. Principle of line and background subtraction. The sensitive line is X_a with the corresponding background, B_a . A second line is X_b with the background, B_b (left part). The key point to adapt time correlation to the IUPAC definition is to select a line S_b so weak that the net line intensity, X_b , may be assimilated to the background B_b (right part). In this case, B_b can be selected near X_a , and we can write that $X_b = B_b$.

integration time, z_{dark} is the dark current in $e \text{ pixel}^{-1} \text{ s}^{-1}$, and σ_{ro} is the readout noise in electron RMS. The shot noise, *i.e.* the noise due to the random nature of the photon emission and collection is, then, equal to $1/z_B \cdot \tau_i$. Note that the integration time is usually fixed by the user, and the software will adjust an exposure time, τ_{exp} within the dynamic range. Also, τ_{exp} will be repeated n times, with $n = \tau_i / \tau_{exp}$.

When using pneumatic nebulization, the flicker noise coefficient, α_B , is in the range 0.005-0.05 (*i.e.* 0.5-5% when expressed in percentage), and z_B ranges from a few to several thousands $e \text{ pixel}^{-1} \text{ s}^{-1}$ when moving from the low uv to the visible part of the spectrum. The value of z_{dark} depends on both the detector and the temperature. At -40°C , z_{dark} is in the range 10^{-2} -100 for a CCD 42-10 from e2v Technologies and for the PerkinElmer Optima 3000 detector, respectively. For the same detectors, the readout noise is 2 and 13 e RMS, respectively.

Similar to the shot noise, the detector noises, *i.e.* the dark current and readout noises, are never correlated when two detectors are used. The photon-related noise should be, then, minimized so as to be negligible compared to the flicker noise. Most of the flicker noise arises from the sample introduction system, which means that the noise should be similar for various signals, leading to a high time correlation. A simple way to minimize the photon-related noise is to increase the integration time. For long integration times, *i.e.* longer than 10 s, it will be easy to minimize the dark current and readout noises. In contrast, the efficiency of minimization of the shot noise will depend on the magnitude of the background intensity. The higher the background, the lower the integration time for the same decrease. In turn, the background intensity

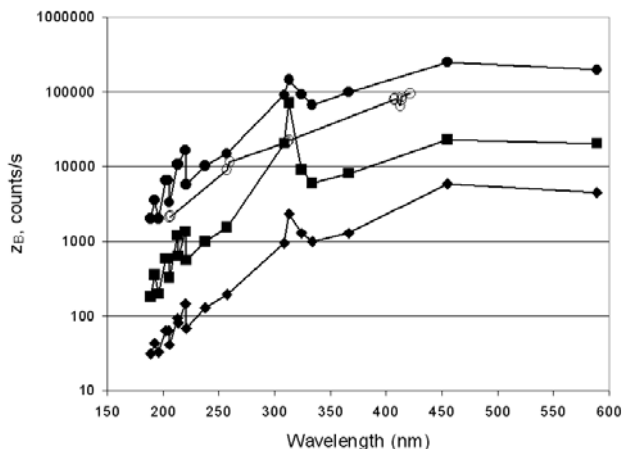


Figure 2. Influence of the operating conditions, power and carrier gas flow rate, and of the viewing mode on the magnitude of the background intensity, z_B , expressed in counts s^{-1} . A PerkinElmer Optima 3000 was used. (◆) radial viewing, 950 W, 0.95 L min^{-1} , (■) axial viewing, 950 W, 0.95 L min^{-1} , (●) axial viewing, 1450 W, 0.60 L min^{-1} , (○) radial viewing, 1300 W, 0.80 L min^{-1} . The first three curves were taken from ref. (19).

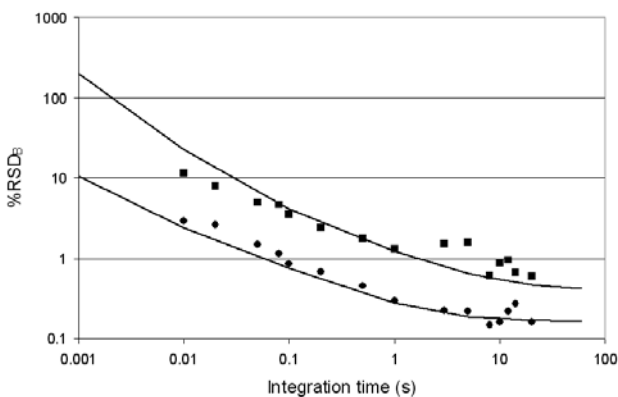


Figure 3. Plot of the experimental $\%RSD_B$ as a function of the integration time using a PerkinElmer Optima 3000 with radial viewing, operating at 1300 W and 0.60 L min^{-1} , for two wavelength regions: (■) 231 nm, (●) 456 nm. Five pixels were used to measure the background intensity. The theoretical curves were computed using equation (18), with a shot noise coefficient, $\beta = 0.13$ (19), a readout noise of 15 e RMS, and a dark current noise of 120 electron $pixel^{-1} s^{-1}$. The value of z_B (counts s^{-1}) and α_B were 7700 and 192000, and 0.004 and 0.0016, for 231 nm and 456 nm, respectively.

depends on i) the wavelength region, with the lowest value for the uv region; ii) the operating conditions, with a high power and a low carrier gas flow rate leading to a high background; and iii) the observation mode, with axial viewing providing a background higher than radial viewing. Note that the background intensity may also be given in counts s^{-1} . In this case, the shot noise is :

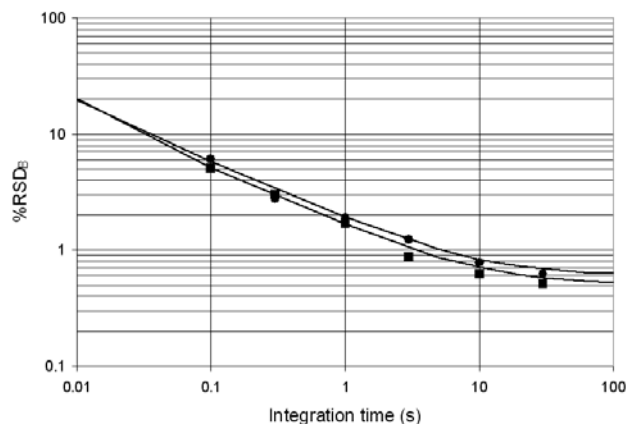


Figure 4. Plot of the experimental $\%RSD_B$ as a function of the integration time using a Jobin-Yvon Activa with radial viewing, operating at 1000 W and 0.75 L min^{-1} , and at wavelengths near 225 nm. (●) e2V 42-10 detector, (■) e2v 30-11 detector. A vertical column binning was used. The theoretical curves were computed using eqn. (18), with a readout noise of 5 e RMS, and a dark current noise of 5 electron $pixel^{-1} s^{-1}$. The values of z_B were 3000 and 4000, for the e2V 42-10 and e2v 30-11 detectors, respectively.

$$\frac{\beta}{z_B \alpha} \tag{19}$$

where β is the shot noise coefficient, usually determined by experiment (19). Examples of background intensities are given in figure 2 for different sets of operating conditions (19) and viewing modes. There is a significant difference in intensity between 250 and 450 nm, *i.e.* around two orders of magnitude. The use of so-called robust conditions, *i.e.* high power and a low carrier gas flow rate, does increase the background intensity.

In order to verify whether the system becomes flicker noise limited, the easiest way is to plot the RSD_B as a function of the integration time using a log-log scale. The shot noise leads, then, to a straight line. When a curvature and a subsequent plateau are observed, the system is then flicker noise limited, and the plot indicates the minimum integration time to obtain possible correlation. Two examples are given in figures 3 and 4. In figure 3, using a PerkinElmer Optima 3000, the RSD_B is plotted for two different wavelengths, 231 and 406 nm, and, therefore, two different values of z_B , 7700 and 192000, respectively. It may be seen that, for a given value of the integration time, the measurements at 406 nm led to a lower value of RSD_B , and a plateau was observed for integration times longer than 30 s.

In figure 4, two different detectors were used on the

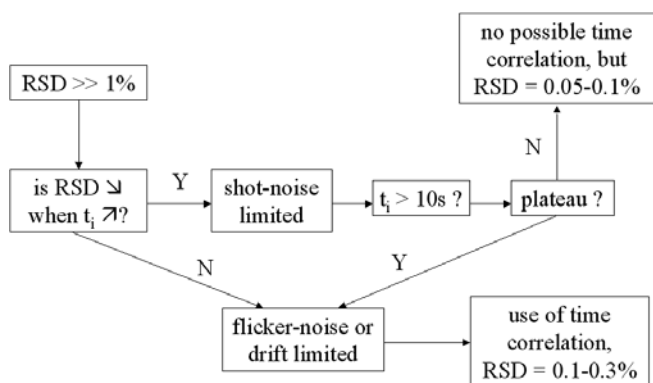


Figure 5. Flow chart of the procedure used to verify whether time correlation can be used to improve LODs by using the $\%RSD_B$ as a function of the integration time.

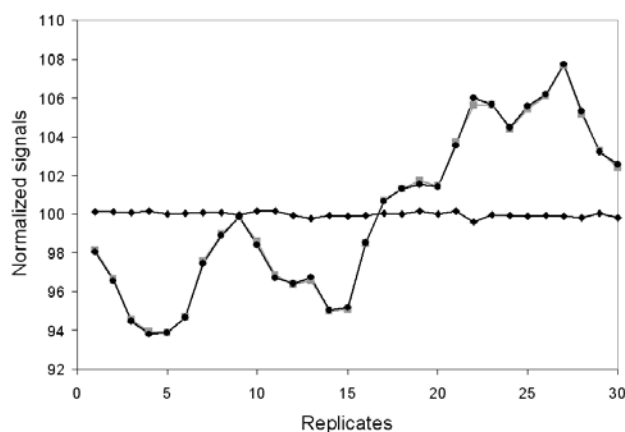


Figure 6. Example of the observation of large flicker noise with a high correlation factor ($\theta = 0.999$). A PerkinElmer Optima 3000 was used at 1100 W and 0.60 L min^{-1} and at wavelengths near 406 nm. Five pixels were used to measure the background intensity. A micronebulizer was used and associated with a cyclonic spray chamber (Micromist from Glass Expansion). The $\%RSD_B$ was 4.2% before subtraction (■, ●) and 0.13% after background subtraction (◆).

Jobin-Yvon Activa system, *i.e.* the e2v 30-11 and e2v 42-10. The major difference between the two detectors was the pixel width, 26 and 13 μm , respectively. Consequently, the spectral bandpass was in a 2 : 1 ratio. However, there was no significant difference between the two curves. A low wavelength was selected, 225 nm, but it was nevertheless possible to observe a plateau above 30 s.

In any case, if a plateau is observed, it can only be for long integration times, usually longer than 30 s.

Procedure

Flow chart

It is very obvious that the measurements must be truly

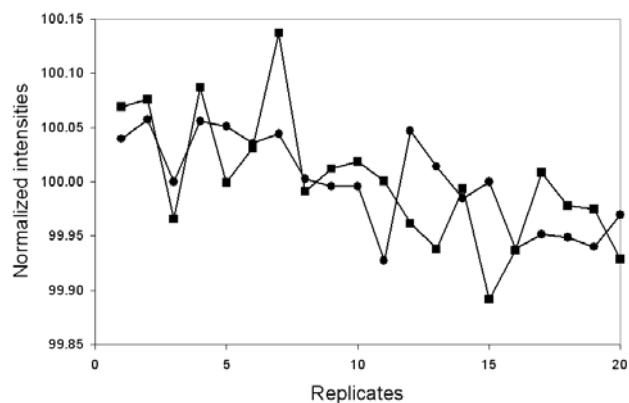


Figure 7. Example of the lack of time correlation because the system was still shot noise limited ($\theta = 0.5$), even for long integration times (30 s). A PerkinElmer Optima 3000 was used at 1300 W and 0.80 L min^{-1} , and at wavelengths near 406 nm. Five pixels were used to measure the background intensity. The $\%RSD_B$ was near 0.5%.

simultaneous, which is not necessarily possible with all CTD detectors. Besides, the same exposure time must be used. The flow chart of the procedure is summarized in figure 5. An improvement in the LOD may be expected for a RSD_B significantly higher than 1%. The first step is to verify whether the system is shot-noise limited or flicker-noise limited. This can be simply verified by plotting RSD_B vs the integration time, as mentioned above. If no decrease is observed, this means that the system is already flicker noise limited, for instance because of a large nebulizer noise. In this case, a high correlation factor may be obtained with a significant reduction in the background noise (figure 6). This is actually the highest improvement.

If RSD_B decreases with the integration time, the system is shot noise limited, and the question is whether or not a plateau is observed for long integration times, *i.e.* > 10 s. If there is no plateau, the system remains shot-noise limited, and there is no possible time correlation; however, the RSD_B can reach very low values, for instance 0.05-0.1%. In figure 7, it may be seen that, even for an integration time of 30 s, there was no correlation between the two backgrounds, and the correlation factor was only equal to 0.5. However, the $\%RSD_B$ was 0.5%, which is an acceptable value.

If a plateau is observed, as in figures 3 and 4, the system is then flicker-noise limited. Alternatively, a small drift may be present, as shown in figure 8, where the correlation factor was 0.965, and the improvement factor was 3. In figure 9, the system was flicker-noise limited, the correlation factor was 0.964, and the improvement

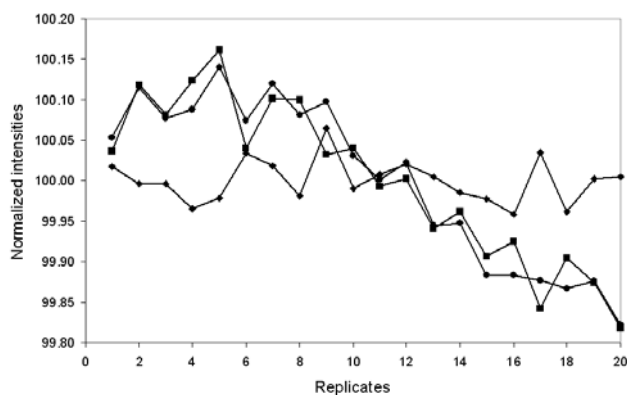


Figure 8. Example of the observation of a small drift, leading to a high correlation factor ($\theta = 0.965$). A PerkinElmer Optima 3000 was used at 1100 W and 0.60 L min⁻¹ and at wavelengths near 406 nm. Five pixels were used to measure the background intensity. The integration time was 30 s. The %RSD_B was 0.1% before subtraction (■, ●) and 0.03% after background subtraction (◆).

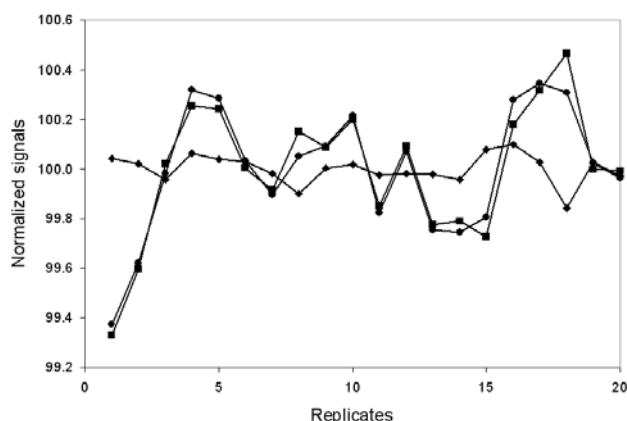


Figure 9. Example of the observation of a flicker-noise limited system with an integration time of 30 s, leading to a high correlation factor ($\theta = 0.974$). A PerkinElmer Optima 3000 was used at 1100 W and 0.60 L min⁻¹ and at wavelengths near 406 nm. Five pixels were used to measure the background intensity. The %RSD_B was 0.26% before subtraction (■, ●), and 0.06% after background subtraction (◆).

factor was 4.

When a plateau is observed, i) a concentration close to a SBR of 1 is selected (*i.e.* near the BEC) ; ii) a large number of replicates is used (20) to measure the fluctuations of X_a , B_a and B_b ; iii) $X_a - B_a$ (or B_b) and $B_a - B_b$ are calculated ; iv) s_{res} is then deduced from $B_a - B_b$; and v) c_L can be then calculated from $X_a - B_a$ and s_{res} . As X_b should be so low that it can be equivalent to the background, B_b , it can be selected at any position, and it is actually convenient to select B_a on one side of the analytical line (X_a) and B_b on the other side (figure 1). For a full efficiency of time correlation, it is important

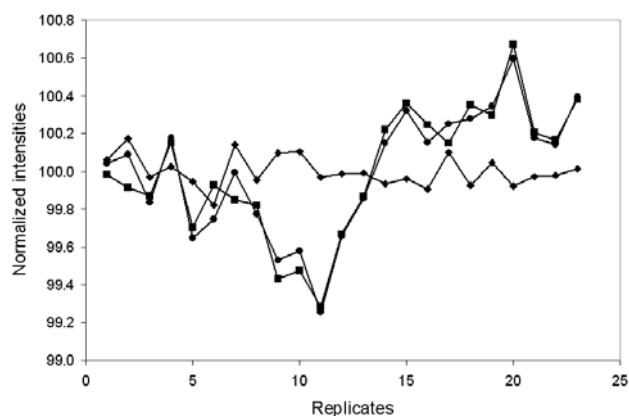


Figure 10. Example of the observation of a flicker-noise limited system with an integration time of 20 s, leading to a high correlation factor ($\theta = 0.96$). A Jobin-Yvon Activa was used at 1000 W and 0.75 L min⁻¹ and at wavelengths near 406 nm. A e2V 42-10 detector with vertical column binning was used. The %RSD_B was 0.33% before subtraction (■, ●) and 0.08% after background subtraction (◆).

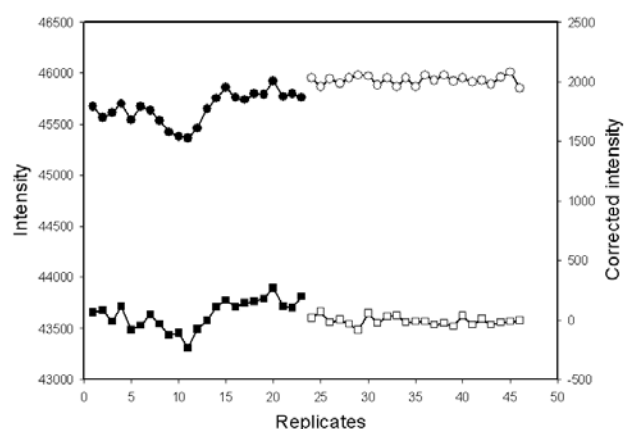


Figure 11. Improvement in the Nd 406 nm LOD, using the same conditions as in figure 10. (●) X_a , (■) B_a , (○) $X_a - B_b$, (□) $B_a - B_b$. The concentration of Nd was 10 ng L⁻¹. The LOD was 2 ng mL⁻¹ before subtraction and 0.5 ng mL⁻¹ after subtraction.

that the values of B_a and B_b be similar so that the standard deviations will have the same magnitude. If not, equation (9) would apply, with a degradation in s_{res} .

Example

A Jobin-Yvon Activa ICP-AES system with radial viewing was used with the standard operating conditions normally selected for LOD determination, *i.e.* a power of 1000 W and a carrier gas flow rate of 0.75 L min⁻¹. An integration time of 20 s was used for the study of the Nd II 406 nm line. The %RSD_B was 0.33% before subtraction, which would be considered in itself an excellent value. However, after background subtraction, the %RSD_B became 0.08% , *i.e.* an outstanding value

(figure 10). Consequently the improvement factor was 4. Practically, a concentration of 10 ng L⁻¹ was used for determination of Nd (figure 11). The LOD was 2 ng mL⁻¹ before correlation and 0.5 ng mL⁻¹ after correlation. Note that Jobin-Yvon considers that the JY Ultima 2 system, equipped with a PMT, provides the best LODs among the Jobin-Yvon ICP-AES systems. For the Ultima 2, using the same line, the LOD was 0.8 ng mL⁻¹, *i.e.* in between the JY Activa LODs with and without time correlation.

Conclusions

Preliminary investigations have indicated that it is possible to adapt the IUPAC LOD definition to time-correlated combination of signals, without the need to redefine a new LOD. This is simply performed by the time-correlated subtraction of two lines and two backgrounds. The only “trick” is to select a classical sensitive line and to subtract from this line another line so weak that its intensity can be comparable to that of a background. As this background can be located anywhere, it is, then, possible to select a background near the sensitive line. It should be mentioned that time correlation between background signals has already been used, but the use of multichannel detection offers the possibility of observing time correlation between every signal, *i.e.* analyte and background signals.

Currently, with the most recent CCD detectors, dark current and readout noises are no longer a limitation. In marked contrast, shot noise, even when using long integration times, may be the limitation, particularly when moving to the UV. Using integration times longer than 1 minute would not be beneficial as the experiment duration would be a penalty, along with the risk of drift. For the time being, it appears that a significant improvement is obtained mostly for long integration times and for the visible region, as the plasma continuum reaches a maximum near 450 nm. Moreover, a large spectral bandpass, *i.e.* several pixels, can be used to collect more photons. In the case of radial viewing, a significant observation zone can be selected (e.g. 5 mm height), by using a 2-D detector and column binning (JY Activa). Currently, it has been possible to observe an improvement factor of up to 5. Better results, in particular in the uv, could be obtained if a more efficient photon collection would be designed.

Acknowledgements

C. Dubuisson and E. Frétel from Jobin-Yvon are gratefully acknowledged for performing experiments on the JY Activa.

References

1. Nomenclature, Symbols, Units and their Usage in Spectrochemical Analysis - II. Data Interpretation, *Pure and Applied Chemistry*, **45**, 99 (1976); *Spectrochim. Acta* **33B**, 241 (1978).
2. J.M. Mermet, *Reviews in Analytical Chemistry, Euroanalysis IX*, Eds. F. Palmisano, L. Sabbatini, P.G. Zambonin, Società Chimica Italiana, Rome, 211 (1997).
3. T.W. Barnard, M.J. Crockett, J.C. Ivaldi, P.L. Lundberg, D.A. Yates, P.A. Levine and D.J. Sauer, *Anal. Chem.*, **65**, 1231 (1993).
4. H. Becker-Ross and S.V. Florek, *Spectrochim. Acta*, **52B**, 1367 (1997).
5. A.T. Zander, R.L. Chien, C.B. Cooper, III and P.V. Wilson, *Anal. Chem.*, **71**, 3332 (1999).
6. J. Houseaux and J.M. Mermet, *J. Anal. At. Spectrom.*, **15**, 979 (2000).
7. S. Luan, R.G. Schleicher, M.J. Pilon, F.D. Bulman and G.N. Coleman, *Spectrochim. Acta*, **56B**, 1143 (2001).
8. J.M. Mermet and J.C. Ivaldi, *J. Anal. Atom. Spectrom.*, **8**, 795 (1993).
9. J.C. Ivaldi and J.F. Tyson, *Spectrochim. Acta*, **51B**, 1443 (1996).
10. S.A. Myers and D.H. Tracy, *Spectrochim. Acta*, **38B**, 1227 (1983).
11. H. Zitter and C. God, *Fresenius Z. Anal. Chem.*, **255**, 1 (1971).
12. Analytical Methods Committee, *Analyst*, **112**, 199 (1987).
13. J.K. Taylor, *Quality assurance of Chemical Measurements*, Lewis Publishers, Chelsea, 1987, chap. 9.
14. M. Thompson, *Analyst*, **113**, 1579 (1988).
15. E. Poussel and J.M. Mermet, *Spectrochim. Acta*, **51B**, 75 (1996).
16. M. Carré, S. Excoffier and J.M. Mermet, *Spectrochim. Acta*, **52B**, 2043 (1997).
17. M. Chausseau, E. Poussel and J.M. Mermet, *Spectrochim. Acta*, **55B**, 1315 (2000).

18. J. Vial and A. Jardy, *Anal. Chem.*, **71**, 2672 (1999).
19. J.C. Ivaldi and J.F. Tyson, *Spectrochim. Acta*, **50B**, 1207 (1995).